Velocity half-sphere model for multiple light scattering in turbid media

S. Menon, Q. Su, and R. Grobe
Intense Laser Physics Theory Unit and Department of Physics, Illinois State University, Normal, Illinois 61790-4560, USA
(Received 1 March 2005; published 11 October 2005)

We extend the traditional diffusion theory by distinguishing between the energy radiance in the forward and backward directions at each point in space. This approach leads to a new effective source for the diffusion equation that is nonzero for an anisotropic light source. It differs significantly from the diffusion theory for short source-detector spacings. We derive an analytical solution for the two lowest-order velocity moments of the radiance.

DOI: 10.1103/PhysRevE.72.041910 PACS number(s): 87.90.+y, 05.60.−k, 42.62.Be

I. INTRODUCTION

The Boltzmann transport equation [1] is used in a wide area of studies. Its applications include the studies of thermal radiation, stellar emission, neutron transport, and light scattering in turbid media [2–4]. In the latter case, the Boltzmann equation models the light by its phase space distribution as a function of the position and the velocity. Despite the lack of a rigorous mathematical derivation from the Maxwell equations, the Boltzmann equation can be motivated phenomenologically based on the particle conservation in phase space [5–7]. Except for a few special cases or special symmetries which lead to reduced dimensional equations, the Boltzmann equation cannot be solved analytically [1]. The most common approach to its solution is through Monte Carlo simulations, in which the photons perform a random-walk-like motion [4].

The Boltzmann equation is equivalent to an infinite but discrete set of coupled differential equations for the velocity moments [8]. In principle, the higher-order moments can be eliminated sequentially, leading to a single differential equation for the zeroth-order moment, the photon density. As an infinite number of velocity moments needs to be eliminated, the resulting differential equation for the photon density is of infinite order. Truncating the discrete set to only the lowest two velocity moments, we obtain two equations. Under additional approximations, they reduce to the usual diffusion equation, which is only of second order in position. The diffusion equation is relatively reliable for highly scattering media at distances far way from the light source. It has the further advantage that, for several situations, fully analytical and easy solutions are available [8,9]. In recent years, the light scattering studies in biological tissues have led to innovative diagnostic techniques in medicine [3,4,10], and the diffusion theory, due to its simplicity, has been used for image reconstruction from experimental scattering data [11].

Despite its many advantages, the diffusion approximation also has several drawbacks. It describes only the time evolution of the first two moments obtained by integration over all velocity directions. It works best for isotropic light distributions and fails in regions close to the source where the directional character of the ejected light is important. A related drawback is the inherent difficulty in describing the dynamics close to medium interfaces. Several works have been devoted to remove these problems [12–21]. One obvious improvement of the lowest-order diffusion theory is to include higher moments. Such improvements are called P_3 or P_5 approximations and show a better agreement with the Boltzmann theory [15,16]. Alternatively, the light distribution close to the source can be separated into its diffusive and the so-called ballistic portions [17–21]. All of these approaches have in common that they describe the light density as a function of the position obtained by the integration over *all* directions of the velocity, therefore being most reliable for nearly isotropic distributions.

In this work, we provide a different approach. To better account for the effect of a directional light source and highly forward scattering media, we introduce two half-sphere integrated moments of the velocity and thus double the number of equations that couple the moments. This approach divides the velocity space into two hemispheres such that the forward and backward scattered light can be described separately at each position. Instead of the two equations, characteristic of the usual diffusion approximation, we obtain four coupled equations. For the special case of an isotropic source, this theory reduces to the standard diffusion theory. For anisotropic light sources, however, this approach improves the accuracy for regions close to the source. In a future communication, we will show that this approach also permits a more accurate treatment of the physical boundaries of the medium, as the forward and backward spheres can be incorporated conveniently into the boundary conditions going beyond the usual Marshak conditions [15,22].

The paper is organized as follows. In Sec. II, we review briefly the approximations leading to the standard diffusion theory. In Sec. III, we derive the mathematical framework for the new set of equations using the half-sphere velocity moments. In Sec. IV, we show how these equations can be solved analytically for a spatially localized source. We will discuss the validity and limitations of the theory by comparing its solutions and those of the standard diffusion with numerical solutions to the Boltzmann equation obtained by Monte Carlo simulations. We will summarize our results and present a short outlook in Sec. V. Detailed mathematical derivations are presented in the Appendixes.

II. VELOCITY FULL-SPHERE MODEL: THE USUAL DIFFUSION APPROXIMATION

In the Boltzmann theory, the light field is described by the six-dimensional phase-space distribution $I(\mathbf{r},\mathbf{\Omega},\omega)$, where $\mathbf{r}$

is the position, $\mathbf{\Omega}$ is the scaled velocity (propagation direction) with $|\mathbf{\Omega}|=1$, and ω is the intensity modulation frequency. In order to obtain the radiance $I(\mathbf{r},\mathbf{\Omega},\omega)$, the radiative transfer (transport) equation

$$(\mathbf{\Omega}\cdot\nabla+\mu_\omega)I(\mathbf{r},\mathbf{\Omega},\omega)=\mu_s\int d\mathbf{\Omega}' p(\mathbf{\Omega}\cdot\mathbf{\Omega}')I(\mathbf{r},\mathbf{\Omega}',\omega) + S(\mathbf{r},\mathbf{\Omega},\omega) \quad (2.1)$$

needs to be solved, where $S(\mathbf{r},\mathbf{\Omega},\omega)$ denotes the spatial and angular characteristics of the light source, $\mu_s(\mu_a)$ is the scattering (absorption) coefficient, and $\mu_\omega\equiv\mu_s+\mu_a+i\omega/c$. The speed of light in the host medium is denoted by c. From now on, we omit the ω dependence in our notation. The conditional probability that an incoming photon with velocity $\mathbf{\Omega}'$ is scattered into the $\mathbf{\Omega}$ direction is denoted by the scattering phase function $p(\mathbf{\Omega}\cdot\mathbf{\Omega}')$. If the scattering is nearly isotropic, the phase function can be approximated by the form

$$p(\mathbf{\Omega},\mathbf{\Omega}')\equiv\frac{1}{4\pi}[1+3g(\mathbf{\Omega}\cdot\mathbf{\Omega}')], \quad (2.2)$$

which is often referred to as the Eddington phase function. The anisotropy parameter g is the average cosine of the scattering angle $g\equiv\langle\mathbf{\Omega}\cdot\mathbf{\Omega}'\rangle$. This phase function is positive only for relatively isotropic scattering $(-1/3<g<1/3)$. For such a medium, the most dominant contribution in $I(\mathbf{r},\mathbf{\Omega})$ is the energy density or fluence (zeroth velocity moment) defined as $\Phi(\mathbf{r})\equiv\int_{4\pi}d\mathbf{\Omega}I(\mathbf{r},\mathbf{\Omega})$ followed by the vector flux (current density) $\mathbf{J}(\mathbf{r})\equiv\int_{4\pi}d\mathbf{\Omega}\mathbf{\Omega}I(\mathbf{r},\mathbf{\Omega})$. In contrast to the velocity half-sphere model discussed below, the two integrals extend over the entire spherical surface of the velocity space. In other words, $\int_{4\pi}d\mathbf{\Omega}=\int_0^{2\pi}d\phi\int_{-1}^{1}d(\cos\theta)$, where θ and ϕ are the polar and azimuthal angles of the vector $\mathbf{\Omega}$. The usual diffusion approximation is characterized by a nearly isotropic moment expansion as

$$I(\mathbf{r},\mathbf{\Omega})\approx\frac{1}{4\pi}[\Phi(\mathbf{r})+3\mathbf{\Omega}\cdot\mathbf{J}(\mathbf{r})]. \quad (2.3)$$

Such an expansion requires $|3\mathbf{\Omega}\cdot\mathbf{J}(\mathbf{r})|\ll\Phi(\mathbf{r})$ to guarantee that $I(\mathbf{r},\mathbf{\Omega})$ remains positive.

For a better comparison with the results of Sec. III, let us quickly review the derivation of the two coupled equations for $\Phi(\mathbf{r})$ and $\mathbf{J}(\mathbf{r})$ from the Boltzmann equation. After integrating Eq. (2.1) over $\int_{4\pi}d\mathbf{\Omega}$, we obtain for the variation in the current density

$$\nabla\cdot\mathbf{J}(\mathbf{r})=-(\mu_\omega-\mu_s)\Phi(\mathbf{r})+q(\mathbf{r}), \quad (2.4)$$

where the zeroth and first velocity moments of source $q(\mathbf{r})$ and $\mathbf{Q}(\mathbf{r})$ (required below) are defined as

$$q(\mathbf{r})\equiv\int_{4\pi}d\mathbf{\Omega}\,S(\mathbf{r},\mathbf{\Omega}), \quad (2.5a)$$

$$\mathbf{Q}(\mathbf{r})\equiv\int_{4\pi}d\mathbf{\Omega}\mathbf{\Omega}S(\mathbf{r},\mathbf{\Omega}). \quad (2.5b)$$

Equation (2.4) is the continuity equation associated with the conservation of particle numbers.

The corresponding equation for $\Phi(\mathbf{r})$ is obtained by multiplying Eq. (2.1) with $\mathbf{\Omega}$ and integrating over $\int_{4\pi}d\mathbf{\Omega}$. Replacing $I(\mathbf{r},\mathbf{\Omega})$ with its approximation Eq. (2.3) and using $\int_{4\pi}d\mathbf{\Omega}\mathbf{\Omega}=\mathbf{0}$ and $\int_{4\pi}d\mathbf{\Omega}\mathbf{\Omega}[\mathbf{\Omega}\cdot\nabla\Phi(\mathbf{r})]=4\pi\nabla\Phi(\mathbf{r})/3$, we obtain what is sometimes called Fick's law,

$$\nabla\Phi(\mathbf{r})=-3(\mu_\omega-g\mu_s)\mathbf{J}(\mathbf{r})+3\mathbf{Q}(\mathbf{r}). \quad (2.6)$$

Equations (2.4) and (2.6) are the two basic equations for the standard diffusion theory. These two coupled equations can be reduced to one if we apply the divergence operator $\nabla\cdot$ to Eq. (2.6) and replace $\nabla\cdot\mathbf{J}$ with the right-hand side of Eq. (2.4). The standard diffusion equation for the fluence $\Phi(\mathbf{r})$ reads

$$[\nabla^2-(i\omega/c+\mu_a)(3i\omega/c+1/D)]\Phi(\mathbf{r}) = -q(\mathbf{r})(3i\omega/c+1/D)+3\nabla\cdot\mathbf{Q}(\mathbf{r}), \quad (2.7)$$

where the diffusion constant is defined as $D\equiv1/[3(\mu_a+\mu_s')]$, and $\mu_s'\equiv(1-g)\mu_s$ is the reduced scattering coefficient. The last source term is only present for an anisotropic source. Please note that the standard diffusion theory only depends on μ_s' (and μ_a) and not on μ_s and g separately. Furthermore, this theory cannot distinguish between a truly isotropic source, $S(\mathbf{\Omega},\mathbf{r})=\delta(\mathbf{r})/(4\pi)$, and a highly collimated source that emits light only along the positive and negative z directions, $S(\mathbf{\Omega},\mathbf{r})=[\delta(\cos\theta+1)+\delta(\cos\theta-1)]\delta(\mathbf{r})/(4\pi)$, as both of these sources lead to $q(\mathbf{r})=\delta(\mathbf{r})$ and $\mathbf{Q}(\mathbf{r})=0$. In a real system, particularly close to the source, the two sources will lead to different fluences and the predictions of Eq. (2.7) cannot be valid.

III. VELOCITY HALF-SPHERE MODEL

In order to provide a more accurate description of anisotropic scattering, we will now distinguish between $I(\mathbf{r},\mathbf{\Omega})$ in the ranges $0\leqslant\theta\leqslant\pi/2$ and $\pi/2<\theta\leqslant\pi$, where θ denotes again the polar angle of the velocity $\mathbf{\Omega}$ with respect to the z axis. We denote the radiances in the ranges $0\leqslant\theta<\pi/2$ by $I_+(\mathbf{r},\mathbf{\Omega})$ and $\pi/2\leqslant\theta<\pi$ by $I_-(\mathbf{r},\mathbf{\Omega})$. The total radiance can be separated as

$$I(\mathbf{r},\mathbf{\Omega})\equiv I_+(\mathbf{r},\mathbf{\Omega})\Theta(\cos\theta)+I_-(\mathbf{r},\mathbf{\Omega})\Theta(-\cos\theta), \quad (3.1)$$

where $\Theta(x)$ is the Heaviside unit step function defined as $\Theta(x)=0$ for $x<0$ and $\Theta(x)=1$ for $x\geqslant0$. Consistent with this separation, we can define the corresponding four velocity moments as

$$\Phi_\pm(\mathbf{r})\equiv\int_{\pm2\pi}d\mathbf{\Omega}\,I(\mathbf{r},\mathbf{\Omega}), \quad (3.2a)$$

$$\mathbf{J}_\pm(\mathbf{r}) \equiv \int_{\pm 2\pi} d\mathbf{\Omega}\mathbf{\Omega} I(\mathbf{r},\mathbf{\Omega}), \tag{3.2b}$$

where the integrations over the velocity half-spheres are defined as $\int_{+2\pi} d\mathbf{\Omega} \equiv \int_0^{2\pi} d\phi \int_0^1 d(\cos\theta)$ and $\int_{-2\pi} d\mathbf{\Omega} \equiv \int_0^{2\pi} d\phi \int_{-1}^0 d(\cos\theta)$. It follows that $\mathbf{J}(\mathbf{r})=\mathbf{J}_+(\mathbf{r})+\mathbf{J}_-(\mathbf{r})$ and $\Phi(\mathbf{r})=\Phi_+(\mathbf{r})+\Phi_-(\mathbf{r})$, however $I(\mathbf{r},\mathbf{\Omega}) \neq I_+(\mathbf{r},\mathbf{\Omega})+I_-(\mathbf{r},\mathbf{\Omega})$. If we express the half-sphere radiances $I_+(\mathbf{r},\mathbf{\Omega})$ and $I_-(\mathbf{r},\mathbf{\Omega})$ in terms of their half-sphere moments, for a linear expansion in $\mathbf{\Omega}$, we obtain

$$I_\pm(\mathbf{r},\mathbf{\Omega}) \approx 2\Phi_\pm(\mathbf{r})/\pi \mp 3J_{\pm z}(\mathbf{r})/\pi + 3\mathbf{\Omega}\cdot\{\mathbf{J}_\pm(\mathbf{r}) + [3J_{\pm z}(\mathbf{r}) \mp 2\Phi_\pm(\mathbf{r})]\hat{\mathbf{z}}\}/(2\pi), \tag{3.3}$$

where $\hat{\mathbf{z}}$ denotes the unit vector along the z direction. Note that Eq. (2.3) cannot be simply generalized to the (incorrect) expansion $I_\pm=[\Phi_\pm+3\mathbf{\Omega}\cdot\mathbf{J}_\pm]/(4\pi)$, and one has to consider the more complicated Eq. (3.3) instead.

In order to better account for the anisotropy of the physical source, the source term in the Boltzmann equation can be separated into the forward and backward directions,

$$S(\mathbf{r},\mathbf{\Omega}) \equiv S_+(\mathbf{r},\mathbf{\Omega})\Theta(\cos\theta) + S_-(\mathbf{r},\mathbf{\Omega})\Theta(-\cos\theta). \tag{3.4}$$

For example, light injected into the medium from an optical fiber along the z axis will strongly emit in the forward direction with no emission into the negative z direction. In this case, the source $S(\mathbf{r},\mathbf{\Omega})$ is nonzero only for $0 \leqslant \theta < \pi/2$ leading to $S_-(\mathbf{r},\mathbf{\Omega})=\mathbf{0}$. Ideally, such a source should not be approximated simply in terms of the moments $\int_{4\pi} d\mathbf{\Omega} S(\mathbf{r},\mathbf{\Omega})$ and $\int_{4\pi} d\mathbf{\Omega}\mathbf{\Omega} S(\mathbf{r},\mathbf{\Omega})$. The impact of the preferred light injection direction is particularly significant if the medium is thin or when the scattering phase function is highly forward peaked as typical for many biological tissues in the visible and IR regions of the spectrum [9].

Equivalently, the two moments of the source can also be defined by their integration over the corresponding velocity half-spheres,

$$q_\pm(\mathbf{r}) \equiv \int_{\pm 2\pi} d\mathbf{\Omega} S(\mathbf{r},\mathbf{\Omega}), \tag{3.5a}$$

$$\mathbf{Q}_\pm(\mathbf{r}) \equiv \int_{\pm 2\pi} d\mathbf{\Omega}\mathbf{\Omega} S(\mathbf{r},\mathbf{\Omega}). \tag{3.5b}$$

For the special case of an isotropic source $[S(\mathbf{r},\mathbf{\Omega}) = f(\mathbf{r})/(4\pi)]$ we have $q_\pm(\mathbf{r})=f(\mathbf{r})/2$ and $\mathbf{Q}_\pm(\mathbf{r}) \equiv \pm f(\mathbf{r})\hat{\mathbf{z}}/4$. We should note that similar to Eq. (2.5), the association of these four moments with the original angular-dependent source $S(\mathbf{r},\mathbf{\Omega})$ is not unique, and one possible way to reconstruct the forward and backward portions of the original source is

$$S_\pm(\mathbf{r},\mathbf{\Omega}) \approx 2q_\pm(\mathbf{r})/\pi \mp 3Q_{\pm z}(\mathbf{r})/\pi + 3\mathbf{\Omega}\cdot\{\mathbf{Q}_\pm(\mathbf{r}) + [3Q_{\pm z}(\mathbf{r}) \mp 2q_\pm(\mathbf{r})]\hat{\mathbf{z}}\}/(2\pi). \tag{3.5c}$$

Let us now use these definitions, to derive the corresponding equations for the four moments $\mathbf{J}_\pm(\mathbf{r})$ and $\Phi_\pm(\mathbf{r})$ from the Boltzmann equation. It turns out, however, that a new set of moments defined as $\Phi(\mathbf{r}) \equiv \Phi_+(\mathbf{r})+\Phi_-(\mathbf{r})$, $\Phi_\Delta(\mathbf{r}) \equiv \Phi_+(\mathbf{r}) - \Phi_-(\mathbf{r})$, $\mathbf{J}(\mathbf{r}) \equiv \mathbf{J}_+(\mathbf{r})+\mathbf{J}_-(\mathbf{r})$, and $\mathbf{J}_\Delta(\mathbf{r}) \equiv \mathbf{J}_+(\mathbf{r})-\mathbf{J}_-(\mathbf{r})$ leads to simpler equations. Furthermore, $\Phi(\mathbf{r})$ and $\mathbf{J}(\mathbf{r})$ provide a direct comparison with the usual diffusion model.

The equations for $\mathbf{J}(\mathbf{r})$ and $\mathbf{J}_\Delta(\mathbf{r})$ can be obtained by inserting the expansion Eq. (3.1) into the Boltzmann equation (2.1) with the phase function Eq. (2.2). The resulting equations for $I_\pm(\mathbf{r},\mathbf{\Omega})$ are

$$(\mathbf{\Omega}\cdot\nabla + \mu_\omega)I_\pm(\mathbf{r},\mathbf{\Omega}) = \mu_s[\Phi(\mathbf{r}) + 3g\mathbf{\Omega}\cdot\mathbf{J}(\mathbf{r})]/(4\pi) + S_\pm(\mathbf{r},\mathbf{\Omega}). \tag{3.6}$$

The right-hand side can be obtained using the identity $\mathbf{\Omega}\cdot\mathbf{\Omega}'=\cos\theta\cos\theta'+\sin\theta\sin\theta'\cos(\phi-\phi')$. Integrating Eq. (3.6) over the velocity half-sphere $\int_{\pm 2\pi} d\mathbf{\Omega}$ and using the relations

$$\int_{\pm 2\pi} d\mathbf{\Omega} = 2\pi, \quad \int_{\pm 2\pi} d\mathbf{\Omega}\mathbf{\Omega} = \pm\pi\hat{\mathbf{z}},$$

and

$$\int_{\pm 2\pi} d\mathbf{\Omega}\mathbf{\Omega}\mathbf{\Omega} = \pm 2\pi(\hat{\mathbf{x}}\hat{\mathbf{x}} + \hat{\mathbf{y}}\hat{\mathbf{y}} + \hat{\mathbf{z}}\hat{\mathbf{z}})/3$$

yields

$$\nabla\cdot\mathbf{J}_\pm(\mathbf{r}) = -\mu_\omega\Phi_\pm(\mathbf{r}) + \mu_s[\Phi(\mathbf{r})/2 \pm 3gJ_z(\mathbf{r})/4] + q_\pm(\mathbf{r}). \tag{3.7}$$

If we add and subtract these two equations from each other, we obtain the two scalar equations

$$\nabla\cdot\mathbf{J}(\mathbf{r}) = -(\mu_\omega - \mu_s)\Phi(\mathbf{r}) + q(\mathbf{r}), \tag{3.8a}$$

$$\nabla\cdot\mathbf{J}_\Delta(\mathbf{r}) = -\mu_\omega\Phi_\Delta(\mathbf{r}) + 3g\mu_s J_z(\mathbf{r})/2 + q_\Delta(\mathbf{r}), \tag{3.8b}$$

where the two source-difference terms are defined as $q_\Delta \equiv q_+ - q_-$ and $\mathbf{Q}_\Delta \equiv \mathbf{Q}_+ - \mathbf{Q}_-$ (used below).

Next we derive the corresponding two vector equations for Φ and Φ_Δ. This derivation is more complicated as, in contrast to the derivation in Sec. II, the integration $\int_{\pm 2\pi} d\mathbf{\Omega}\mathbf{\Omega}$ does not separate the required terms of the defined variables. Instead of the usual procedure, the velocity half-sphere geometry requires us to integrate Eq. (3.6) with respect to $\int_{\pm 2\pi} d\mathbf{\Omega}\mathbf{\Omega}\, P_5(\cos\theta)$, where P_5 is the fifth-order Legendre polynomial. We remark that instead of $P_5(\cos\theta)$ any Legendre polynomial of odd order $\geqslant 5$ would have led to the same set of final equations. Inserting the linear expansion of Eq. (3.3) into the Boltzmann equation (3.6), we obtain the following form: $\mathbf{H}_{1\pm}+\mathbf{H}_{2\pm}+\mathbf{H}_{3\pm}=\mathbf{H}_{4\pm}+\mathbf{H}_{5\pm}$, where the ten terms are

$$\mathbf{H}_{1\pm} \equiv \int_{\pm 2\pi} d\mathbf{\Omega}\mathbf{\Omega} P_5(\cos\theta)(\mathbf{\Omega}\cdot\nabla)(\mathbf{\Omega}\cdot 3/2\pi\{\mathbf{J}_\pm(\mathbf{r}) + [3J_{\pm z}(\mathbf{r}) \mp 2\Phi_\pm(\mathbf{r})]\hat{\mathbf{z}}\}) = \mathbf{0}, \tag{3.9a}$$

$$\mathbf{H}_{2\pm} \equiv \int_{\pm 2\pi} d\boldsymbol{\Omega}\boldsymbol{\Omega} P_5(\cos\theta)\boldsymbol{\Omega}\cdot(\boldsymbol{\nabla}\{[2\Phi_\pm(\mathbf{r}) \mp 3J_{\pm z}(\mathbf{r})]/\pi\} + 3\mu_\omega/2\pi\{\mathbf{J}_\pm(\mathbf{r}) + [3J_{\pm z}(\mathbf{r}) \mp 2\Phi_\pm(\mathbf{r})]\hat{\mathbf{z}}\}) = \pm\pi(\boldsymbol{\nabla}\{[2\Phi_\pm(\mathbf{r}) \mp 3J_{\pm z}(\mathbf{r})]/\pi\} + 3\mu_\omega/2\pi\{\mathbf{J}_\pm(\mathbf{r}) + [3J_{\pm z}(\mathbf{r}) \mp 2\Phi_\pm(\mathbf{r})]\hat{\mathbf{z}}\})\cdot[\alpha\hat{\mathbf{x}}\hat{\mathbf{x}} + \alpha\hat{\mathbf{y}}\hat{\mathbf{y}} + 2\beta\hat{\mathbf{z}}\hat{\mathbf{z}}], \tag{3.9b}$$

$$\mathbf{H}_{3\pm} \equiv \int_{\pm 2\pi} d\boldsymbol{\Omega}\boldsymbol{\Omega} P_5(\cos\theta)\mu_\omega\{[2\Phi_\pm(\mathbf{r}) \mp 3J_{\pm z}(\mathbf{r})]/\pi\} = \mathbf{0}, \tag{3.9c}$$

$$\mathbf{H}_{4\pm} \equiv \int_{\pm 2\pi} d\boldsymbol{\Omega}\boldsymbol{\Omega} P_5(\cos\theta)[\mu_s/(4\pi)\Phi(\mathbf{r}) + 2q_\pm(\mathbf{r})/\pi \mp 3Q_{\pm z}(\mathbf{r})/\pi] = \mathbf{0}, \tag{3.9d}$$

$$\mathbf{H}_{5\pm} \equiv \int_{\pm 2\pi} d\boldsymbol{\Omega}\boldsymbol{\Omega} P_5(\cos\theta)\boldsymbol{\Omega}\cdot([3g\mu_s/(4\pi)\mathbf{J}(\mathbf{r})] + 3\{\mathbf{Q}_\pm(\mathbf{r}) + [3Q_{\pm z}(\mathbf{r}) \mp 2q_\pm(\mathbf{r})]\hat{\mathbf{z}}\}/(2\pi)) = \pm\pi([3g\mu_s/(4\pi)\mathbf{J}(\mathbf{r})] + 3\{\mathbf{Q}_\pm(\mathbf{r}) + [3Q_{\pm z}(\mathbf{r}) \mp 2q_\pm(\mathbf{r})]\hat{\mathbf{z}}\}/(2\pi))\cdot[\alpha\hat{\mathbf{x}}\hat{\mathbf{x}} + \alpha\hat{\mathbf{y}}\hat{\mathbf{y}} + 2\beta\hat{\mathbf{z}}\hat{\mathbf{z}}]. \tag{3.9e}$$

The two constants are defined as $\alpha \equiv \int_0^1 dx(1-x^2)P_5(x) = 13/192$ and $\beta \equiv \int_0^1 dx x^2 P_5(x) = -1/192$. We refer the reader to Appendix A for detailed derivations of these integrals. Due to the special form of the pre-factor $\boldsymbol{\Omega}P_5(\cos\theta)$ in the integrand, the Boltzmann equation reduces to the two vector equations $\mathbf{H}_{2\pm} = \mathbf{H}_{5\pm}$. Making a dot product with the tensor $[\hat{\mathbf{x}}\hat{\mathbf{x}}/\alpha + \hat{\mathbf{y}}\hat{\mathbf{y}}/\alpha + \hat{\mathbf{z}}\hat{\mathbf{z}}/(2\beta)]$ yields

$$\boldsymbol{\nabla}[2\Phi_\pm(\mathbf{r}) \mp 3J_{\pm z}(\mathbf{r})] = -\frac{3}{2}\mu_\omega\{\mathbf{J}_\pm(\mathbf{r}) + [3J_{\pm z}(\mathbf{r}) \mp 2\Phi_\pm(\mathbf{r})]\hat{\mathbf{z}}\} + \frac{3\mu_s g}{4}\mathbf{J}(\mathbf{r}) + 3/2\{\mathbf{Q}_\pm(\mathbf{r}) + [3Q_{\pm z}(\mathbf{r}) \mp 2q_\pm(\mathbf{r})]\hat{\mathbf{z}}\}. \tag{3.10}$$

Subtracting and adding these two equations, we obtain

$$\boldsymbol{\nabla}[2\Phi(\mathbf{r}) - 3J_{\Delta z}(\mathbf{r})] = -(3i\omega/c + 1/D)/2\mathbf{J}(\mathbf{r}) + 3/2\mu_\omega[2\Phi_\Delta(\mathbf{r}) - 3J_z(\mathbf{r})]\hat{\mathbf{z}} + 3/2\mathbf{Q}(\mathbf{r}) + 3/2[3Q_z(\mathbf{r}) - 2q_\Delta(\mathbf{r})]\hat{\mathbf{z}}, \tag{3.11a}$$

$$\boldsymbol{\nabla}[2\Phi_\Delta(\mathbf{r}) - 3J_z(\mathbf{r})] = -3/2\mu_\omega\{\mathbf{J}_\Delta(\mathbf{r}) + [3J_{\Delta z}(\mathbf{r}) - 2\Phi(\mathbf{r})]\hat{\mathbf{z}}\} + 3/2\{\mathbf{Q}_\Delta(\mathbf{r}) + [3Q_{\Delta z}(\mathbf{r}) - 2q(\mathbf{r})]\hat{\mathbf{z}}\}. \tag{3.11b}$$

This set of four coupled equations (3.8) and (3.11) forms the basic equations for the four moments Φ, Φ_Δ, $\mathbf{J}$, and $\mathbf{J}_\Delta$. In contrast to Eqs. (2.4) and (2.6) for $\mathbf{J}$ and Φ, this set is more complicated due to the terms $3J_{\Delta z}$ and $3J_z$ on the left-hand side of Eq. (3.11). Taking the vector character of the variables into account, we have a set of eight coupled partial differential equations. In Sec. II, we showed that the two first-order differential equations for $\mathbf{J}$ and Φ could be combined to a single second-order equation for Φ. Following this approach, one could expect (in the absence of the terms $3J_{\Delta z}$ and $3J_z$) that the four coupled equations (3.8) and (3.11) can be converted into two coupled second-order differential equation for Φ and Φ_Δ. In Appendix B, we show that three unexpected major simplifications occur. First, the two terms $3J_{\Delta z}$ and $3J_z$ do not cause problems and can be eliminated effectively with the introduction of a new variable. Second, the equation for Φ is effectively decoupled from Φ_Δ. Third, it is only of second (and not of fourth) order. The final equation for $\Phi(\mathbf{r})$ takes the remarkably simple form

$$[\boldsymbol{\nabla}^2 - (i\omega/c + \mu_a)(3i\omega/c + 1/D)]\Phi(\mathbf{r}) = -q(\mathbf{r})(3i\omega/c + 1/D) + 3\,\boldsymbol{\nabla}\cdot\mathbf{Q}(\mathbf{r}) + S_{\text{new}}(\mathbf{r}). \tag{3.12a}$$

Except for the new sourcelike term S_{new}, defined as

$$S_{\text{new}}(\mathbf{r}) \equiv 3\frac{1}{\mu_\omega}\partial^2/\partial z^2\left[q(\mathbf{r}) - \tfrac{3}{2}Q_{\Delta z}(\mathbf{r})\right] - 3\frac{1}{\mu_\omega}\boldsymbol{\nabla}^2[q(\mathbf{r}) - 2Q_{\Delta z}(\mathbf{r})] - \frac{3}{2}\frac{1}{\mu_\omega}\partial/\partial z\,\boldsymbol{\nabla}\cdot\mathbf{Q}_\Delta(\mathbf{r}), \tag{3.12b}$$

this equation is completely identical to the one obtained from the standard diffusion theory, Eq. (2.7). As the new effective source term of Eq. (3.12) is computed from the spatial derivative of the original source term, it is spatially more localized than the original source. We therefore would expect that its impact is only significant for distances close to the original source. We also note that there are spatial regions in which this term can be negative, therefore effectively reducing the source strength on the right-hand side. We will return to this analysis in Sec. IV where we will discuss the solutions of these equations. If the original source is fully isotropic with $S(\mathbf{r}) = f(\mathbf{r})/(4\pi)$, $[q(\mathbf{r}) = f(\mathbf{r})$ and $\mathbf{Q}_\Delta(\mathbf{r}) \equiv \hat{\mathbf{z}}f(\mathbf{r})/2]$, we have $S_{\text{new}} = 0$ as expected.

We also present in Appendix B the corresponding differential equation for the difference variable $\Phi_\Delta(\mathbf{r})$, which, however, is more complicated as it couples to $\Phi(\mathbf{r})$. The final solutions for $\Phi(\mathbf{r})$ and $\Phi_\Delta(\mathbf{r})$ can be inserted into Eqs. (3.8) and (3.11) to solve for $J(\mathbf{r})$ and $J_\Delta(\mathbf{r})$. These four solutions can be converted into the original variables $\Phi_\pm$ and $\mathbf{J}_\pm$ to find the total radiance $I(\mathbf{r},\boldsymbol{\Omega})$ via Eqs. (3.3) and (3.1).

IV. COMPARISON OF THE TWO MODELS WITH THE BOLTZMANN THEORY

A. General solutions to the velocity half-sphere and full-sphere models

Let us now discuss the general solutions to Eqs. (2.7) and (3.12). In the usual diffusion model, the source is characterized by its first and second moments, $q(\mathbf{r})$ and $\mathbf{Q}(\mathbf{r})$, whereas the half-sphere model requires the eight quantities $q(\mathbf{r})$, $q_\Delta(\mathbf{r})$, $\mathbf{Q}(\mathbf{r})$, and $\mathbf{Q}_\Delta(\mathbf{r})$ as defined in Eqs. (3.5). To provide an analytical solution, we assume here for simplicity that the source is frequency-independent and localized such that its spatial dependence is given by $S(\mathbf{r},\mathbf{\Omega})=S(\mathbf{\Omega})\delta(\mathbf{r})$. The solution associated with a spatially extended source could be obtained easily from the localized source solution due to the linearity of the diffusion equation. From now on, we omit the spatial dependence and denote the angular moments by the eight numbers q, q_Δ, $\mathbf{Q}$, and $\mathbf{Q}_\Delta$.

Both equations can be written in the compact form $[\boldsymbol{\nabla}^2-\kappa^2]\Phi(\mathbf{r})=-\boldsymbol{L}\delta(\mathbf{r})$, where the parameter κ is defined as $\kappa^2\equiv(i\omega/c+\mu_a)(3i\omega/c+1/D)$. The operator for the full-sphere model is

$$\boldsymbol{L}_f = q(3i\omega/c + 1/D) - 3\mathbf{Q}\cdot\boldsymbol{\nabla}, \tag{4.1}$$

whereas the operator for the half-sphere model takes the form

$$\boldsymbol{L}_h = q(3i\omega/c + 1/D) - 3\mathbf{Q}\cdot\boldsymbol{\nabla} + 3/\mu_\omega(q-2Q_{\Delta z})(\boldsymbol{\nabla}^2-\partial^2/\partial z^2) + 3/(2\mu_\omega)(Q_{\Delta x}\partial/\partial x + Q_{\Delta y}\partial/\partial y)\partial/\partial z. \tag{4.2}$$

The solution of the two equations is possible as $\boldsymbol{L}$ commutes with $\boldsymbol{\nabla}^2$ and we can readily write the solution as $\Phi(\mathbf{r})=\boldsymbol{L}G(\mathbf{r})$, where $G(\mathbf{r})=\exp(-\kappa r)/(4\pi r)$ is the Green's function for $[\boldsymbol{\nabla}^2-\kappa^2]G(\mathbf{r})=-\delta(\mathbf{r})$. The application of the differential operators is straightforward and we obtain for the full- and half-sphere models

$$\Phi_f(\mathbf{r}) = \boldsymbol{L}_f G(\mathbf{r}) = q(3i\omega/c + 1/D)G(\mathbf{r}) + 3\mathbf{Q}\cdot\mathbf{r}G(\mathbf{r})(\kappa+1/r)/r, \tag{4.3a}$$

$$\Phi(\mathbf{r}) = \boldsymbol{L}_h G(\mathbf{r}) = \Phi_f(\mathbf{r}) + 3/\mu_\omega(q-2Q_{\Delta z})G(\mathbf{r})[\kappa^2\sin^2\vartheta - (\kappa/r+1/r^2)\times(3\cos^2\vartheta-1)] + 3/(2\mu_\omega)G(\mathbf{r})(3/r^2+3\kappa/r+\kappa^2)\sin\vartheta\cos\vartheta(Q_{\Delta x}\cos\varphi + Q_{\Delta y}\sin\varphi), \tag{4.3b}$$

where ϑ and φ denote the polar and azimuthal angles of the position vector $\mathbf{r}$. Both solutions differ by the last two terms in Eq. (4.3b), which vanish if the source is fully isotropic.

B. Comparison with the Boltzmann solution for a directed light source

In order to compare the accuracy of the standard diffusion theory and the half-sphere model with the Boltzmann theory, we have to choose a specific source. For simplicity, let us assume an angularly collimated source, given by $S(\mathbf{r},\mathbf{\Omega},\boldsymbol{\omega})=\delta(\cos\theta-1)\delta(\mathbf{r})/(2\pi)$, leading to $q=1$, $q_\Delta=1$, $\mathbf{Q}=(0,0,1)$, and $\mathbf{Q}_\Delta=(0,0,1)$. Note that a solution for an angularly collimated point source is a Green's function which can be used to obtain a solution for any arbitrary source. For light scattering in an infinite medium, we obtain in the limit $\omega\to 0$

$$\Phi(\mathbf{r}) = 1/DG(\mathbf{r}) + 3\cos\vartheta G(\mathbf{r})(k+1/r) - 3/\mu_T G(\mathbf{r})[k^2\sin^2\vartheta - (3\cos^2\vartheta-1)(k/r+1/r^2)], \tag{4.4}$$

where $k\equiv\sqrt{\{3[\mu_s(1-g)+\mu_a]\mu_a\}}$. The difference between the half- and full-sphere approaches is best illustrated for the special case of vanishing absorption, $\mu_a=0$. In this case, the final expression simplifies considerably and we obtain

$$\Phi(\mathbf{r}) = 3\mu_s(1-g)/(4\pi r) + 3\cos\vartheta/(4\pi r^2) + 3/\mu_s(3\cos^2\vartheta - 1)/(4\pi r^3). \tag{4.5}$$

The first two terms are the solutions for the full-sphere model. The last term is due to the separation into velocity half-spheres. It is interesting to note that Eq. (4.5) appears to have a multipole expansion form. However, to confirm this conjecture, we would need to include higher-order terms in expanding the phase function and the radiance Eq. (3.3), which is still quite a nontrivial task. For $r\to\infty$, both solutions are identical, however at short distances, where the $1/r^3$ term becomes relevant, the two theories differ. This is illustrated in Fig. 1, where the contour plots of $\Phi(\mathbf{r})/\mu_s^2$ in the $y=0$ plane are displayed for a relatively isotropic ($g=0.2$) and highly forward ($g=0.9$) scattering media. As only the (monopole) term depends on the anisotropy factor in Eq. (4.5), g determines the relative importance of the effect of the angular collimation of the source as well as the maximum source-detector spacing, at which the correction to the diffusion theory due to the $1/r^3$ term can be detected. The traditional diffusion approximation depends only on $\mu_s(1-g)$ while the correction term depends on μ_s alone in Eq. (4.5). This suggests that a separate determination of μ_s and g is in principle possible with our new theory [18,19,21], but not possible in the standard diffusion theory [15]. Such a separation involves measurements at short and long source-detector separations.

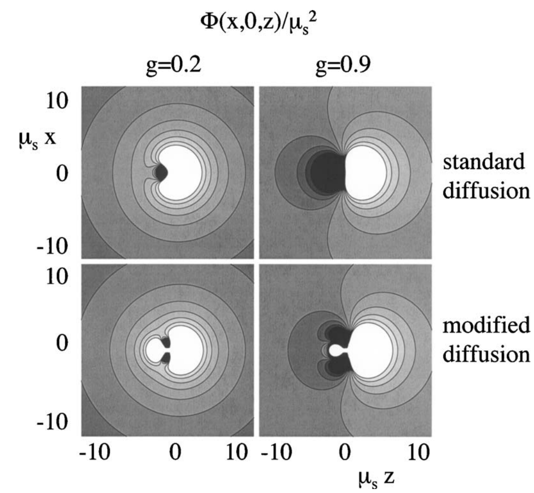

FIG. 1. Contour plot of the steady-state fluence $\Phi(\mathbf{r})/\mu_s^2$ in the $y=0$ plane as predicted by the diffusion and modified diffusion theories of Eq. (4.5). The source is located at $\mathbf{r}=\mathbf{0}$ and ejects light along the positive z direction. The dark areas denote (unphysical) negative fluences.

The third term increases the fluence along the forward ($\vartheta\approx 0$) direction and surprisingly also along the backward ($\vartheta\approx\pi$) direction, whereas the light along the two perpendicular directions ($\vartheta\approx\pi/2$) is reduced as $(3\cos^2\vartheta-1)$ turns negative, as shown by the dark regions. Thus the major improvement over the diffusion solution is along the forward and backward directions. As the last term is uniquely associated with the extra source term, denoted as S_{new} in Eq. (3.12), it is clear that for ϑ close to $\pi/2$ it is negative, acting there as an effective photon sink. The condition $3\mu_s(1-g)/(4\pi r)+3\cos\vartheta/(4\pi r^2)+3/\mu_s(3\cos^2\vartheta-1)/(4\pi r^3)<0$ is possible if μ_s is sufficiently small, pointing to a direct breakdown of the theory. However, this is not so unexpected, as in the limit $r\to 0$, even the fluence $\Phi(\mathbf{r})$ predicted by the standard diffusion theory turns negative if $\vartheta>\pi/2$. A comparison of the two contour plots within each row in Fig. 1 shows how the modified diffusion (half-sphere model) reduces the extension of those regions for which the diffusion theory is inapplicable as indicated by the dark colors. Clearly, this improvement is a result of approximating a collimated source by the anisotropic expansion (3.5c) as compared to the usual diffusion expansion.

In order to test the accuracy of these solutions, we have performed a large scale Monte Carlo (MC) simulation [22–24] to the Boltzmann Eq. (2.1) with 10^6 photons, each of which performed a random walk with a random distance s distributed according to $P(s)=\exp(-\mu_s s)/\mu_s$ and with random scattering angle distributed according to a Henyey-Greenstein phase function $P_{\text{HG}}(\mathbf{\Omega}\cdot\mathbf{\Omega}')=(1-g^2)/\{4\pi(1+g^2-2g\mathbf{\Omega}\cdot\mathbf{\Omega}')^{3/2}\}$. The MC Boltzmann photon distribution is time-dependent, $\Phi_B(\mathbf{r},t)$, and was calculated for a pulsed light source that emitted photons at time $t=0$. In order to obtain the corresponding steady-state distribution ($\omega=0$) from the time-dependent simulation, the resulting photon distribution determined at each time t was integrated in time according to $\Phi_B(\mathbf{r})=\int_0^T d\tau\Phi_B(\mathbf{r},T-\tau)\exp[-c\mu_a(T-\tau)]$, which describes the steady state associated with a time-independent source if the total integration time T is large enough.

In Fig. 2, we compare the photon density in the forward and backward detection directions with respect to the laser source as a function of the detector-source spacing r. Graphed is the integral $F(r)$ or $B(r)\equiv 2\pi r^2\int d\vartheta\sin\vartheta\Phi(r,\vartheta)$, where the integration limits for the polar angle are $0<\vartheta<\pi/4$ for the front $[F(r)]$ detector and $3\pi/4<\vartheta<\pi$ for the back $[B(r)]$ detector, respectively. In the Monte Carlo simulation, these quantities are the probability densities to find a photon on the corresponding semispherical surface area with radius of curvature r. The analytical predictions for these two radial densities can be obtained easily, using $\int d\vartheta\sin\vartheta=[1-1/\sqrt{(2)}]$, $\int d\vartheta\sin\vartheta\cos(\vartheta)=\pm 1/4$, $\int d\vartheta\sin\vartheta\cos^2(\vartheta)=[4-\sqrt{(2)}]/12$, and $\int d\vartheta\sin\vartheta\sin^2(\vartheta)=2/3-5\sqrt{(2)}/12$, for $0<\vartheta<\pi/4$ and $3\pi/4<\vartheta<\pi$, respectively,

$$F(r)\equiv 2\pi r^2\int d\vartheta\sin\vartheta\Phi(\mathbf{r})$$
$$=2\pi r^2([1-1/\sqrt{(2)}]/D+3/4(k+1/r)-3/\mu_T\{k^2[2/3-5\sqrt{(2)}/12]-\sqrt{(2)}/4(k/r+1/r^2)\})G(\mathbf{r}),\quad(4.6a)$$

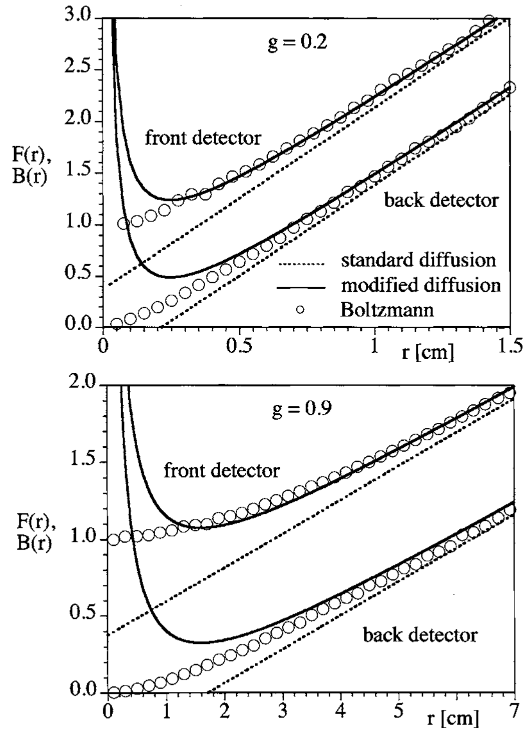

FIG. 2. The angle-integrated fluence detected along the forward and backward directions as a function of the source detector spacing r for $g=0.2$ (top) and $g=0.9$ (bottom). The source, located at $\mathbf{r}=\mathbf{0}$, was highly collimated along the z axis. The open circles denote the Monte Carlo results, the solid line is the modified, and the dotted line is the traditional diffusion solution. The Monte Carlo data were obtained from averages over 10^6 photon paths. Each photon path was recorded for 400 m, which was necessary to obtain converged results for this absorption-free medium ($\mu_s=5$ cm^{-1} and $\mu_a=0$).

$$B(r)\equiv 2\pi r^2\int d\vartheta\sin\vartheta\Phi(\mathbf{r})$$
$$=2\pi r^2([1-1/\sqrt{(2)}]/D-3/4(k+1/r)-3/\mu_T\{k^2[2/3-5\sqrt{(2)}/12]-\sqrt{(2)}/4(k/r+1/r^2)\})G(\mathbf{r}).\quad(4.6b)$$

Figure 2 was obtained for $\mu_s=5$ cm^{-1} and $\mu_a=0$. The agreement with the exact data (circles) obtained from the Monte Carlo simulation extends to much smaller source-detector spacings ($\approx 1/\mu_s'$) for the modified theory in the front as well as back detection directions. We should mention that in order to obtain the theoretical results for the highly forward scattering case, $g=0.9$, the standard and modified diffusion theories were computed for effective scattering parameters $f=g^2$, $\mu_s(1-f)=0.95$ cm^{-1}, and $\tilde{g}\equiv g/(g+1)=0.47$, associated with the predictions based on the δ-Eddington scattering phase function [17,25] of the form $P_{\delta\text{-}E}(\mathbf{\Omega}\cdot\mathbf{\Omega}')\equiv\{2f\delta(1-\mathbf{\Omega}\cdot\mathbf{\Omega}')+(1-f)[1+3\tilde{g}(\mathbf{\Omega}\cdot\mathbf{\Omega}')]\}/4\pi$, and not Eq. (2.2). Note that because we assumed a δ-function form of the source, both fluences Eq. (4.3) diverge for small values of r. The fluence when integrated over the entire surface is finite. In Fig. 2, however, we plot the fluence over a small area and thus the divergence due to the modified solution is present

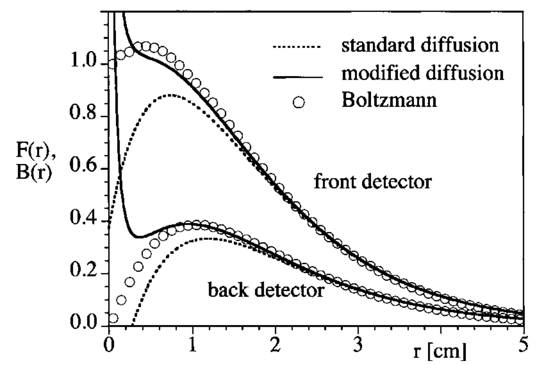

FIG. 3. The light distribution detected along the forward and backward directions as a function of the source detector spacing r for an absorptive medium. The Monte Carlo data were obtained from averages over 10^6 photon paths. Each photon path was recorded for 0.1 m, which was sufficient for convergence ($\mu_s = 5\ \mathrm{cm}^{-1}$, $g=0.2$, and $\mu_a = 0.1\ \mathrm{cm}^{-1}$).

because of the $1/r^3$ correction that is absent in the usual diffusion solution.

In Fig. 3, we extend the comparison for a relatively strongly absorptive medium. We choose again $\mu_s = 5\ \mathrm{cm}^{-1}$ and $g=0.2$, however $\mu_a = 0.1\ \mathrm{cm}^{-1}$. Even though each individual photon path decays due to the frequent scatterings, after a length of $\approx 1/\mu_a = 10$ cm, the effect of absorption in the steady-state distribution is visible at much shorter source-detector spacings. Mathematically, this is reflected by the fact that the exponential decay factor in Eq. (4.4) is $k = \sqrt{\{3\mu_a[\mu_a + (1-g)\mu_s]\}}$, which for our parameters is $1.1\ \mathrm{cm}^{-1}$ and 11 times larger than μ_a. As a result, the fluence falls off rapidly after an initial rise that cannot be predicted accurately by both theories. However, similarly to the absorption-free case, the modified diffusion theory improves the standard theory.

V. SUMMARY AND OUTLOOK

We have examined a conceptually new approach to study the multiple scattering of light in turbid media. In order to take the effect of the anisotropy of the light source into account, we have separated the velocity space into two hemispheres relative to the main injection direction of the source. The theory describes the spatial distribution of four velocity moments obtained with respect to these hemispheres. Quite remarkably, it turns out that the resulting four coupled equations for these moments can be reduced to a simple second-order equation for the total fluence. This equation differs from the standard diffusion theory by an additional source-like term which can also act like a sink in directions perpendicular to the main light injection directions. Due to this remarkably simple outcome, even this more complicated approach leads to fully analytical solutions for the fluence. We have established the improvement of this new approach over the standard diffusion theory by a comparison with the numerical solution of the Boltzmann equation.

The next logical step to further improve this theory could be to divide the phase space into even smaller velocity regions and to obtain the corresponding equations for these new moments. This approach could provide even higher-order corrections in $1/r$ to the full Boltzmann solution. At present, however, even a numerical implementation of such a scheme is extremely challenging even if the phase function remains restricted to the form given by Eq. (2.2). As a first step, one could examine the two-dimensional Boltzmann equation for which the velocity directions are characterized by a single variable and therefore could be more easily divided up into four velocity regions. In the limiting case of only one spatial direction, the Boltzmann equation can be solved fully analytically for the fluence along the positive and negative directions.

Another improvement to the velocity half-sphere model can be obtained by taking into account higher moments of the scattering phase function, which in this treatment was restricted to the first two moments in Eq. (2.2). In the traditional diffusion theory, only the first two moments of the phase function can be incorporated, which limits its validity near boundaries, particularly in highly forward scattering media [15,16]. On the other hand, the velocity half-sphere model has the dual advantage of better incorporating the boundary conditions and taking also higher moments of the phase function into account. Such complications have been intentionally avoided in this article to keep the focus on the analytically solvable systems.

One could also try to combine the present approach with one in which the ballistic light is separated first from the Boltzmann equation before the diffusion approximation is invoked [17–21]. We have recently shown that a ballistic correction can improve the spatial regions close to an anisotropic source [20,21]. This ballistic correction could further improve the half-sphere model leading possibly to a very accurate description of light scattering near a source and near a plane boundary.

ACKNOWLEDGMENTS

This work has been supported by the NSF. We also acknowledge support from Research Corporation, BLV, and NCSA.

APPENDIX A

The derivation of Eqs. (3.9) was based on the following three vector identities:

$$\int_{\pm 2\pi} d\mathbf{\Omega}\,\mathbf{\Omega} P_5(\cos\theta) = \mathbf{0}, \tag{A1}$$

$$\int_{\pm 2\pi} d\mathbf{\Omega}\,\mathbf{\Omega} P_5(\cos\theta)\mathbf{\Omega}\cdot\mathbf{V} = \pm[\pi V_x(I_0 - I_2)\hat{\mathbf{x}} + \pi V_y(I_0 - I_2)\hat{\mathbf{y}} + 2\pi V_z I_2 \hat{\mathbf{z}}], \tag{A2}$$

$$\int_{\pm 2\pi} d\mathbf{\Omega}\,\mathbf{\Omega} P_5(\cos\theta)(\mathbf{\Omega}\cdot\mathbf{V}_1)(\mathbf{\Omega}\cdot\mathbf{V}_2) = \mathbf{0} \tag{A3}$$

for arbitrary constant vectors $\mathbf{V}$, $\mathbf{V}_1$, and $\mathbf{V}_2$. The numerical constants I_0, I_1, I_2, I_3 are defined as

$$I_0 = \int_0^1 dx x^0 P_5(x) = 1/16, \quad \text{(A4a)}$$

$$I_1 = \int_0^1 dx x P_5(x) = 0, \quad \text{(A4b)}$$

$$I_2 = \int_0^1 dx x^2 P_5(x) = -1/192, \quad \text{(A4c)}$$

$$I_3 = \int_0^1 dx x^3 P_5(x) = 0. \quad \text{(A4d)}$$

The first equality (A1) follows if we express $\mathbf{\Omega}$ in Cartesian coordinates:

$$\int_{\pm 2\pi} d\mathbf{\Omega}\mathbf{\Omega} P_5(\cos\theta) = \int_{\pm 2\pi} d\mathbf{\Omega}(\sin\theta\cos\phi\hat{\mathbf{x}} + \sin\theta\sin\phi\hat{\mathbf{y}} + \cos\theta\hat{\mathbf{z}})P_5(\cos\theta) = \hat{\mathbf{z}}\int_{\pm 2\pi} d\mathbf{\Omega}\cos\theta P_5(\cos\theta) = \mathbf{0} \quad \text{(A5)}$$

because $\int_0^{2\pi} d\phi \cos\phi = \int_0^{2\pi} d\phi \sin\phi = 0$.

To show the second equality (A2) is a little bit more involved,

$$\int_{\pm 2\pi} d\mathbf{\Omega}\mathbf{\Omega} P_5(\cos\theta)\mathbf{\Omega}\cdot\mathbf{V} = \int_{\pm 2\pi} d\mathbf{\Omega}(\sin\theta\cos\phi\hat{\mathbf{x}} + \sin\theta\sin\phi\hat{\mathbf{y}} + \cos\theta\hat{\mathbf{z}})P_5(\cos\theta) \times (\sin\theta\cos\phi V_x + \sin\theta\sin\phi V_y + \cos\theta V_z). \quad \text{(A6)}$$

Using $\int_0^{2\pi} d\phi \cos\phi\sin\phi = 0$, $\int_0^{2\pi} d\phi \cos^2\phi = \int_0^{2\pi} d\phi \sin^2\phi = \pi$, and $\int_0^{2\pi} d\phi = 2\pi$ we observe that only the "diagonal" terms are nonzero

$$\begin{aligned}\int_{\pm 2\pi} d\mathbf{\Omega}\mathbf{\Omega} P_5(\cos\theta)\mathbf{\Omega}\cdot\mathbf{V} &= \int_{\pm 2\pi} d\mathbf{\Omega}(V_x\sin^2\theta\cos^2\phi\hat{\mathbf{x}} + V_y\sin^2\theta\sin^2\phi\hat{\mathbf{y}} + V_z\cos^2\theta\hat{\mathbf{z}})P_5(\cos\theta) \\ &= 2\pi\int_{\pm} dx(V_x\sin^2\theta/2\hat{\mathbf{x}} + V_y\sin^2\theta/2\hat{\mathbf{y}} + V_z\cos^2\theta\hat{\mathbf{z}})P_5(\cos\theta) \\ &= 2\pi\int_{\pm} dx[V_x(1-x^2)/2\hat{\mathbf{x}} + V_y(1-x^2)/2\hat{\mathbf{y}} + V_z x^2\hat{\mathbf{z}}]P_5(x) \\ &= \pm 2\pi[V_x(I_0 - I_2)/2\hat{\mathbf{x}} + V_y(I_0 - I_2)/2\hat{\mathbf{y}} + V_z I_2\hat{\mathbf{z}}]. \end{aligned} \quad \text{(A7)}$$

The proof of the last equality (A3) follows in a similar way:

$$\begin{aligned}&\int_{\pm 2\pi} d\mathbf{\Omega}\mathbf{\Omega} P_5(\cos\theta)(\mathbf{\Omega}\cdot\mathbf{V}_1)(\mathbf{\Omega}\cdot\mathbf{V}_2) \\ &= \int_{\pm} d(\cos\theta)P_5(\cos\theta)\pi\hat{\mathbf{x}}(V_{1x}V_{2z}\sin^2\theta\cos\theta + V_{1z}V_{2x}\sin^2\theta\cos\theta) \\ &\quad + \int_{\pm} d(\cos\theta)P_5(\cos\theta)\pi\hat{\mathbf{y}}(V_{1y}V_{2z}\sin^2\theta\cos\theta + V_{1z}V_{2y}\sin^2\theta\cos\theta) \\ &\quad + \int_{\pm} d(\cos\theta)P_5(\cos\theta)2\pi\hat{\mathbf{z}}(V_{1z}V_{2z}\cos^3\theta) \\ &= \int_{\pm} d(\cos\theta)P_5(\cos\theta)\pi\hat{\mathbf{x}}[V_{1x}V_{2z}(1-\cos^2\theta)\cos\theta + V_{1z}V_{2x}(1-\cos^2\theta)\cos\theta] \\ &\quad + \int_{\pm} d(\cos\theta)P_5(\cos\theta)\pi\hat{\mathbf{y}}[V_{1y}V_{2z}(1-\cos^2\theta)\cos\theta + V_{1z}V_{2y}(1-\cos^2\theta)\cos\theta] \\ &\quad + \int_{\pm} d(\cos\theta)P_5(\cos\theta)2\pi\hat{\mathbf{z}}[V_{1z}V_{2z}\cos^3\theta] = \mathbf{0}, \end{aligned} \quad \text{(A8)}$$

where we have used $\int_0^{2\pi} d\phi \cos^3\phi = \int_0^{2\pi} d\phi \sin^3\phi = \int_0^{2\pi} d\phi \cos^2\phi\sin\phi = \int_0^{2\pi} d\phi \sin^2\phi\cos\phi = 0$.

APPENDIX B

Let us discuss how to derive the equations for $\Phi(\mathbf{r})$ appearing in Eq. (3.12) and a new equation for $\Phi_\Delta(\mathbf{r})$ that is not included in the main text. Let us define the auxiliary variable $Y \equiv 2\Phi_\Delta - 3J_z$ as a measure of the anisotropy. Using the z component of Eq. (3.11b), we get

$$J_{\Delta z}(\mathbf{r}) = \frac{1}{2}\Phi(\mathbf{r}) - \frac{1}{6\mu_\omega}\frac{\partial}{\partial z}Y(\mathbf{r}) + \frac{1}{2\mu_\omega}[2Q_{\Delta z}(\mathbf{r}) - q(\mathbf{r})]. \quad \text{(B1)}$$

Substituting Eq. (B1) into Eq. (3.11a) and (3.11b), we obtain

$$\begin{aligned}\mathbf{J}(\mathbf{r}) = (3i\omega/c + 1/D)^{-1}\Bigg[&-\nabla\Phi(\mathbf{r}) - \frac{1}{\mu_\omega}\frac{\partial}{\partial z}\nabla Y(\mathbf{r}) + 3\mu_\omega Y(\mathbf{r})\hat{\mathbf{z}} \\ &+ \frac{3}{\mu_\omega}[2\nabla Q_{\Delta z}(\mathbf{r}) - \nabla q(\mathbf{r})] + 3\mathbf{Q}(\mathbf{r}) + 3[3Q_z(\mathbf{r}) - 2q_\Delta(\mathbf{r})]\hat{\mathbf{z}}\Bigg] \end{aligned} \quad \text{(B2)}$$

$$\mathbf{J}_\Delta(\mathbf{r}) = -\frac{2}{3\mu_\omega}\nabla Y(\mathbf{r}) + \left[\frac{1}{2\mu_\omega}\frac{\partial}{\partial z}Y(\mathbf{r}) + \frac{1}{2}\Phi(\mathbf{r})\right]\hat{\mathbf{z}} + \frac{1}{\mu_\omega}\mathbf{Q}_\Delta(\mathbf{r}) - \frac{1}{2\mu_\omega}q(\mathbf{r})\hat{\mathbf{z}}. \tag{B3}$$

Note that Eq. (B2) is a generalized form of Fick's law. If $Y=0$, the rightmost term in Eq. (B2) is equal to zero and this expression would reduce to the one given by Eq. (2.6). Note that Eq. (3.8b) can be rewritten in terms of Y as $\nabla\cdot\mathbf{J}_\Delta+\mu_\omega Y/2+J_z/2(3i\omega/c+1/D)=q_\Delta$. Substituting $\mathbf{J}_\Delta$ from Eq. (B3) in this equation and using J_z from the third component of the vector equation (B2), we obtain

$$[\nabla^2-3\mu_\omega^2]Y(\mathbf{r}) = -6\mu_\omega q_\Delta(\mathbf{r}) - 3\partial q(\mathbf{r})/\partial z + 9\mu_\omega Q_z(\mathbf{r}) + 3/2\,\nabla\cdot\mathbf{Q}_\Delta(\mathbf{r}) + 9/2\,\partial Q_{\Delta z}(\mathbf{r})/\partial z. \tag{B4}$$

Applying the gradient operator on Eq. (B2), replacing $\nabla\cdot\mathbf{J}(\mathbf{r})$ by Eq. (3.8a), and replacing the term $[\nabla^2-3\mu_\omega^2]Y$ by the right-hand side of Eq. (B4), we obtain

$$\begin{aligned}[\nabla^2-(i\omega/c+\mu_a)(3i\omega/c+1/D)]\Phi(\mathbf{r}) &= -q(\mathbf{r})(3i\omega/c+1/D) + 3\nabla\cdot\mathbf{Q}(\mathbf{r}) \\ &\quad + 3\frac{1}{\mu_\omega}\partial^2/\partial z^2[q(\mathbf{r})-3/2Q_{\Delta z}(\mathbf{r})] - 3\frac{1}{\mu_\omega}\nabla^2[q(\mathbf{r}) \\ &\quad - 2Q_{\Delta z}(\mathbf{r})] - \frac{3}{2}\frac{1}{\mu_\omega}\partial/\partial z\,\nabla\cdot\mathbf{Q}_\Delta(\mathbf{r})\end{aligned} \tag{B5}$$

which completes the derivation of Eq. (3.12).

The corresponding equation for $\Phi_\Delta(\mathbf{r})$ can be obtained by rewriting Eq. (B4) as

$$\begin{aligned}2c[\nabla^2-3\mu_\omega^2]\Phi_\Delta(r) &= [\nabla^2-3\mu_\omega^2]3J_z(\mathbf{r}) - 6\mu_\omega q_\Delta(\mathbf{r}) \\ &\quad - 3\partial q(\mathbf{r})/\partial z + 9\mu_\omega Q_z(\mathbf{r}) \\ &\quad + 3/2\,\nabla\cdot\mathbf{Q}_\Delta(\mathbf{r}) + 9/2\,\partial Q_{\Delta z}(\mathbf{r})/\partial z.\end{aligned} \tag{B6}$$

Using the z component of the vector equation (B2), we obtain

$$\begin{aligned}[\nabla^2-3\mu_\omega^2]\Phi_\Delta(\mathbf{r}) &= -\frac{3}{2}[\nabla^2-3\mu_\omega^2](3i\omega/c+1/D)^{-1}\partial/\partial z\Phi(\mathbf{r}) \\ &\quad + \frac{3}{2}(3i\omega/c+1/D)^{-1}\Bigg\{\Bigg[(3i\omega/c+1/D)/3 \\ &\quad - \frac{1}{\mu_\omega}(\partial^2/\partial z^2-3\mu_\omega^2)\Bigg] \\ &\quad \times[-6\mu_\omega q_\Delta(\mathbf{r})3\partial q(\mathbf{r})/\partial z + 9\mu_\omega Q_z(\mathbf{r}) \\ &\quad + 3/2\,\nabla\cdot\mathbf{Q}_\Delta(\mathbf{r}) + 9/2\,\partial Q_{\Delta z}(\mathbf{r})/\partial z] - [\nabla^2 \\ &\quad - 3\mu_\omega^2]\Bigg[\frac{3}{\mu_\omega}[2\partial Q_{\Delta z}(\mathbf{r})/\partial z - \partial q(\mathbf{r})/\partial z] \\ &\quad + 3Q_z(\mathbf{r}) + 3[3Q_z(\mathbf{r}) - 2q_\Delta(\mathbf{r})]\Bigg]\Bigg\}.\end{aligned} \tag{B7}$$

Note that in contrast to Eq. (3.12), $\Phi_\Delta(\mathbf{r})$ is coupled to $\Phi(\mathbf{r})$ and therefore requires its solution on the right-hand side.

[1] S. Chandrasekhar, *Radiative Transfer* (University Clarendon Press, Oxford, 1950).
[2] A. Ishimaru, *Wave Propagation and Scattering in Random Media*, Vols. 1 and 2 (Academic, New York, 1978).
[3] V. V. Tuchin, Phys. Usp. **40**, 495 (1997).
[4] See articles in *Optical Biomedical Diagnostics*, edited by V. V. Tuchin (SPIE, Bellingham, 2002).
[5] M. C. W. van Rossum and T. M. Nieuwenhuizen, Rev. Mod. Phys. **71**, 313 (1999).
[6] S. Menon, Q. Su, and R. Grobe, Phys. Rev. E **65**, 051917 (2002).
[7] S. Menon, Q. Su, and R. Grobe, Phys. Rev. E **68**, 046614 (2003).
[8] P. Morse and H. Feshbach, *Methods of Theoretical Physics* (McGraw Hill, New York, 1953), Chap. 12.
[9] W. M. Star, in *Optical-Thermal Response of Laser-Irradiated Tissue*, edited by A. J. Welch and M. J. C. van Gemert (Plenum, New York, 1995), pp. 131–206.
[10] A. Yodh and B. Chance, Phys. Today **48**(3), 34 (1995).
[11] B. B. Das, F. Liu, and R. R. Alfano, Rep. Prog. Phys. **60**, 227 (1997).
[12] L. Perelman, J. Wu, I. Itzkan, and M. Feld, Phys. Rev. Lett. **72**, 1341 (1994); L. T. Perelman, J. Wu, Y. Wang, I. Itzkan, R. R. Dasari, and M. S. Feld, Phys. Rev. E **51**, 6134 (1995).
[13] A. Polishchuk, M. Zevallos, F. Liu, and R. Alfano, Phys. Rev. E **53**, 5523 (1996).
[14] D. J. Durian and J. Rudnick, J. Opt. Soc. Am. A **14**, 235 (1997).
[15] E. L. Hull and T. H. Foster, J. Opt. Soc. Am. A **18**, 584 (2001).
[16] A. C. Selden, Phys. Med. Biol. **49**, 3017 (2004).
[17] S. A. Prahl, Ph.D. thesis, University of Texas at Austin (1998).
[18] V. Venugopalan, J. S. You, and B. J. Tromberg, Phys. Rev. E **58**, 2395 (1998).
[19] C. K. Hayakawa, B. Y. Hill, J. S. You, F. Bevilacqua, J. Spanier, and V. Venugopalan, Appl. Opt. **43**, 4682 (2004).
[20] S. Menon, Q. Su, and R. Grobe, Opt. Lett. **30**, 1542 (2005).
[21] S. Menon, Q. Su, and R. Grobe, Phys. Rev. Lett. **94**, 153904 (2005).
[22] R. C. Haskell, L. O. Svaasand, T. Tsoy, T. Feng, M. S. McAdams, and B. J. Tromberg, J. Opt. Soc. Am. A **11**, 2727 (1994).
[23] L. H. Wang, S. L. Jacques, and L. Q. Zheng, Comput. Methods Programs Biomed. **47**, 131 (1995).
[24] D. A. Boas, J. P. Culver, J. J. Stott, and A. K. Dunn, Opt. Express **10**, 159 (2002).
[25] S. A. Carp, S. A. Prahl, and V. Venugopalan, J. Biomed. Opt. **9**, 632 (2004).